Molecular Crystals and Liquid Crystals

ISSN: 1542-1406 (Print) 1563-5287 (Online) Journal homepage: http://www.tandfonline.com/loi/gmcl20

Preparation and characterization of solid lipid microparticles with liquid crystal structure

Y. Miao, B. Jia, M. Chen & W. Zhang

To cite this article: Y. Miao, B. Jia, M. Chen & W. Zhang (2016) Preparation and characterization of solid lipid microparticles with liquid crystal structure, Molecular Crystals and Liquid Crystals, 633:1, 110-122, DOI: 10.1080/15421406.2016.1177899

To link to this article: http://dx.doi.org/10.1080/15421406.2016.1177899

MOLECULAR CRYSTALS AND LIQUID CRYSTALS
2016, VOL. 633, 110–122
http://dx.doi.org/10.1080/15421406.2016.1177899

Taylor & Francis
Taylor & Francis Group

Preparation and characterization of solid lipid microparticles with liquid crystal structure

Y. Miao[a], B. Jia[a], M. Chen[b], and W. Zhang[a]

[a]School of Perfume and Aroma Technology, Shanghai Institute of Technology, Fengxian district Shanghai, People's Republic of China; [b]Research and development, JALA Corporation Xuhui District, Shanghai, China

ABSTRACT

The aim of this study was the preparation and characterization of solid lipid microparticles (SLMs) with liquid crystal structure. In order to observe the morphology of SLMs, environmental emission scanning electron microscopy was employed. And the structure of particles measured by polarized light optical microscopy and X-ray diffraction. Differential scanning calorimetry (DSC) was used to measure the crystallinity. Karl Fischer Titration were used to measure the micro amount of water content. The optimal formation was prepared. The influence of homogenization rate, emulsification temperature, concentration of NaCl, co-emulsifier type and concentration on particle size was discussed.

KEYWORDS

Co-emulsifier; liquid crystal; NaCl; solid lipid microparticle

1. Introduction

Liquid crystals (LC) in emulsion droplets have been a topic of interest for many years. Liquid crystals represented an intermediate state of order between the solid and the liquid, and had the characterizations of both crystals and liquids. They can be obtained by two mechanisms [1]. The liquid crystals formed by an increase of temperature were known as thermotropic liquid crystals. Another is obtained by the addition of amphiphilic organic materials in which part of the constituent molecules favors one solvent, normally water, while the other part does not was named aslyotropic liquid crystal. Generally, LC has the following shapes [2]: disk-like molecules, which form discotic liquid crystals; amphiphilic compounds, which form layered columnar or cubic phases in the pure state and in solution. Currently the lyotropic liquid crystals had been prevalent in pharmaceutical and cosmetic while the thermotropic liquid crystals were mainly used in the electro-optic display and not considered further [3]. Lyotropic LC was usually classified as lamellar, cubic hexagonal, or tetragonal [4]. The different type LLC consisted of different shapes of micelles in different ways. The lamellar liquid crystal was formed by double molecular layers laminated together. The cubic hexagonal liquid crystals consist of the rod-like micelles in the parallel arrangement. The structure unit of cubic LC was the ellipsoid or short rod-like micelles which were arranged according to the cubic lattice. The pharmaceutical compounds have been increasingly characterized by their lyotropic liquid crystalline states. T. Rades [5] found that fenoprofen sodium can form a lamellar structure with a layer spacing of 2.8 nm. The phase diagram for the binary system nafcillin sodium-water was determined using differential scanning calorimetry (DSC) and

CONTACT W. Zhang zhwanp@126.com
Color versions of one or more of the figures in the article can be found online at www.tandfonline.com/gmcl.

polarized light microscopy and the result showed that a striated texture consisting of rod like micelles of indefinite length arranged side by side in a hexagonal pattern. Ko [6] studied the Tetragonal crystal of cyclosporine in different solvents such as chloroform, acetone or methanol solutions. Many features of LLC that are advantageous for dermal application of cosmetic have been reported [7,8]. In internal structure of LLCs, hydrophilic and hydrophobic parts could incorporate water soluble drug and oil soluble drug, respectively [9]. The role of lyotropic liquid crystals in emulsion stabilization has been also addressed in recent papers [10]. In contrast to conventional emulsions, liquid crystals films surround emulsion droplets and prevent their coalescence. Recently, biocompatible, highly stable emulsions using a lamellar phase as the whole dispersing medium were prepared [11].

Another noteworthy field was the solid lipid microparticles. SLMs were developed as an alternative colloidal system to liposomes, microemulsions, and polymeric particles [12,13]. SLMs, the first generation of lipid particles, are produced by replacing the liquid lipid (oil) of an o/w emulsion by a solid lipid or a blend of solid lipids, i.e. the lipid particle matrix being solid at both room and body temperature [14]. Lipid particles have been proposed as an alternative to colloidal delivery systems, emulsions and liposomes, presenting flexibility with respect to adjusting the size of the desired particle. Amongst the lipids, phospholipids, triacylglycerols, waxes, fatty acids or their mixtures can be used [15]. Priscilla Chui Hong Wong et al. [16] use cetyl alcohol as lipid in determination of Solid State Characteristics on Solid lipid microparticles. Fernando Eustáquio Matos-Jr et al. [17] use Vegetable glycerol monostearate 90 as lipid in producing solid lipid microparticles loaded with ascorbic acid. Vivek Ramshankar Yadav et al. [18] use Soya lecithin, stearic acid and palmitic acid as lipids in preparing and evaluating the anti-inflammatory activity of solid lipid microparticles (SLMs) of curcumin. Compared to the traditional colloidal systems, SLMs avoid the disadvantages [19,20], such as limited physical stability, aggregation, drug leakage on storage, cytotoxicity of polymers etc., instead showing low cytotoxicity, drug targeting, excellent biocompatibility and biodegradability [21–23]. SLMs have been investigated for various pharmaceutical and cosmetic application, e.g. parenteral, peroral and dermal administration [13]. Due to the occlusive properties of solid lipid microparticles, an increased skin hydration effect is observed. Enhancement of chemical stability after incorporation into the particles was proven for many cosmetic actives. Advantages of liquid crystals applications in cosmetics that can be pointed out: the visual appearance, because of the thermochromism; the incorporation of active components inside liquid crystals or even in formulations where they are present, the ability of preventing photo and thermal degradation; potential of promoting water retention in the stratum corneum (SC) and so increasing the cutaneous hydration; and, finally promoting actives-controlled release. Nowadays, it is already known that some lipids of the intercellular area, as the ceramides, assume the lamellar liquid crystalline structures contributing this way also to the cutaneous hydration [24]. Above all, solid lipid microparticles with liquid crystal structure can combine the advantages of both SLM and liquid crystal structure. However, the solid lipid microparticles with the liquid crystal structure were studied by few researchers. The SLMs with liquid crystal offer several advantages for encapsulation of active components including improved physical stability, protection to chemical degradation and precise control over release, furthermore, it usually exhibit high water holding capacity due to the liquid crystal.

In the present study, our aim is to prepare the solid lipid microparticles with liquid crystal. Optimize the formation consist of C16-C18 as solid lipid and C22APG as surfactants by the polarized light optical microscopy. Environmental emission scanning electron microscopy was employed to observe the SLMs morphology. And the structure of particles identified by

X-ray diffraction. The crystallinity and micro amount of water content were measured by Differential scanning calorimetry and Karl Fischer Titration. The influence of homogenization rate, emulsification temperature, concentration of NaCl, co-emulsifier type, and concentration on particle size was studied.

2. Materials and methods

2.1. Materials

C_{22}APG was used as the main surfactant of liquid crystal structure supplied by SEPPIC, France. C16-C18 Normal Mixed Alcohols(1618) and steareth-21(S-21, Eumulgin®S 21) which respectively act as the solid lipid and co-emulsifier, were purchased from BASF. The other two co-emulsifiers were glyceryl monostearate (GMS, Crode) and ceteareth-20 (C-20, Laibo, Shanghai). The caprylic/capric triglyceride (GTCC) was purchased from BASF. The NaCl was supplied by Tansoolechemical company. The water used throughout the experiments was deionized.

2.2. Preparation of formulation

Emulsions were prepared by the ordinary emulsification method. Briefly, The aqueous phase and the oil phase(C_{22}APG, C_{16}-C_{18}Normal Mixed Alcohols as the lipid, the co-emulsifier) separately heated at about 80°C.Then the oil phase was added to the water phase using a homogenizer (IKA®T-10 basic Ultra-Turrax®, Germany) at a certain rate. The homogeneous time is about 2 min. After that, the obtained emulsion was cooled down under stirring (IKA-RW20 digital) at 910 Kr/min.

2.3. Determination of particle size

The particle size distribution and mean droplet diameter of diluted emulsions were measured by a commercial dynamic light scattering (DLS) device (Malvern Zetasizer Nano ZSUK). Mean particle diameters were reported as "Z-average" diameters (the scattering intensity-weighted mean diameter), which were calculated from the signal intensity versus particle diameter data normalized to size increments using Mie Theory.

2.4. Polarized light optical microscopy

Microscopic analysis of the investigated samples was conducted in order to gain information about the liquid crystal characteristics of the emulsion.LC can be observed under crossed polarizers due to the birefringence of LC. An optical polarizing microscope (Olympus *R* BX 50, Olympus Optical Co., Tokyo, Japan) with a computer was used in the study. Relevant images were digitalized using a camera attached to the microscope (Olympus DP12, Japan) and computer software (Olympus DP-Soft, Version 3.2). An appropriate amount of freshly prepared emulsion was placed onto the microscopic slide. A coverslip was placed on the sample by ensuring that no air or bubbles were trapped between the sample and cover slip.

2.5. Environmental emission scanning electron microscopy

Shape and surface morphology of the microparticles with liquid crystal were examined by environmental emission scanning electron microscopy(ESEM) (FEI company, Quanta200 FEG, Holland). Prior to analysis, the sample was diluted with deionized water, placed on a double side carbon tape mounted onto analuminium stud, and air-dried. Then, images were obtained at ×30,000 magnification at an excitation voltage of 5 kV.

2.6. X-ray diffraction

A RIGAKU X-ray scattering diffractometer (RIGAKU, D/MAX 2550 VB/PC, Japan) with a copper anode ($\lambda = 0.154056$ nm) and a Goniometer detector was utilized to study phase and structure of the lipids. The scanning rate was fixed at 0.002°/min and The X-ray diffraction patterns were obtained from 2θ of 0.5°–10°. The Ka1 and Ka2 wavelengths were 0.154060 and 0.154439 nm, respectively, and the relative intensity of Ka1/Ka2 was equal to 2.

2.7. Differential scanning calorimetry

Differential scanning calorimetry (DSC) was measured on a DSC Q2000 apparatus (TA Instruments, USA). The thermo grams of bulk lipid, steareth-21, C22APG and lyophilized emulsion were recorded. Samples (∼2–5 mg) sealed in standard aluminum pans were kept under isothermal condition at 2°C for 10 min. An empty pan was used as a reference. DSC scans were recorded at heating rate of 10°C·min^{-1}. All samples were heated from20°Cup to 100°C.

2.8. Karl Fischer titration

A Karl Fischer Titration (ZSD-2, Anting Electronics, Shanghai, China) was used to measure micro amount of water content which presence in lamellar liquid crystalline. K·F reagent was calibrated by using the redistilled water. In this study, water reacts with iodine and sulfur dioxide 10 µL (W') of redistilled water was taken by using syringe and then injected into the titration cell where iodine and water react for coulometric titration, the number exhibited at the screen was A', which represents the amount of Karl Fischer reagent that the titration consumed. The water content was calculated by following equation:

$$F = \frac{W'}{\mathrm{A}'},$$

$$Water\ content\% = \mathrm{A} \times \frac{F}{W} \times 100\%.$$

Where, F represents the amount of water that each milliliter of KF reagent consumed, W represents the weight of the sample (mg), A represents the amount of KF reagent that the sample consumed.

3. Results and discussion

3.1. Preparation of solid lipid microparticles with liquid crystal

It is well established that the liquid crystals formed by surfactants in water were driven by hydrophobic interactions [25,26]. Lipid particles have been proposed as an alternative to

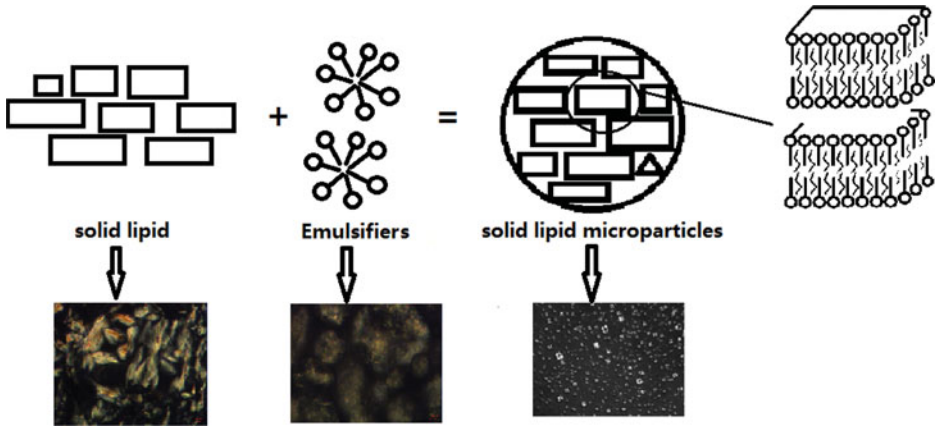

Figure 1. The formation mechanism of solid lipid microparticles with liquid crystal structure.

colloidal delivery systems, emulsions and liposomes [27], presenting flexibility with respect to adjusting the size of the desired particle. Amongst the lipids, phospholipids, triacylglycerols, waxes, fatty acids or their mixtures can be used [28].

In this study, the lipid particles consist of C16–C18 fatty alcohols as solid lipids and C22APG as surfactants. Although the intrinsic order within a LC material can be controlled by external parameters, the ordering can also be controlled internally through weak interactions to create more complex structures that add functionality to the material. One approach is to obtain self-assembled structures from a variety of different molecules. Another is to form phase-segregated structures of "block" molecules of longer polymers and smaller molecules on the nanometer and micrometer scale. The control of intermolecular interactions within these structures is critical because several competing effects are at work [29]. This study used16–C18 fatty alcohols to form phase-segregated structures of "block" molecules of solid lipid microparticles (SLMs). C16–C18 is specific oil capable of forming critical order; moreover, surfactants can also form critical order by micelles as shown in Fig. 1. When C16–C18 fatty alcohols combine with the main surfactant and co-surfactants, they present a stable critical order together with the formation of the lamellar liquid crystals (evidence in article 3.2.2). The mechanism of formation of particles is shown in Fig. 1. Formation of liquid crystals by C22APG under different conditions is shown in Fig. 2. Phenomenological investigation of the samples by polarization microscopy revealed different anisotropic textures within the SLMs. In general, the liquid crystals of C22APG in water were characterized by the radial configuration, a characteristic feature of lamellar liquid crystals. Lamellar phase has ordered structure folded by many parallel planes of the surfactant molecular duplication.

Figs. 2a–c show that at different high emulsification temperatures, the SLMs consist of liquid crystal and exhibit a uniform distribution. However, at lower temperatures, liquid crystals are shiny and scattered; and distorted with irregular shapes. Thus, the high temperature favored the distribution.

The addition of co-emulsifier could affect the dispersion of C22 APG in the water. Fig. 2d–f exhibit SLMs with different co-emulsifiers. The system containing glyceryl monostearate (GMS) as co-emulsifier contributed to form large and light liquid crystal for which the boundary conditions are planar at spherical surfaces, the defect structure and the defect configuration. Other co-emulsifiers such as ceteareth-20 and steareth-21 showed negligible effect on the array of the micelles. Only the amount and size were affected.

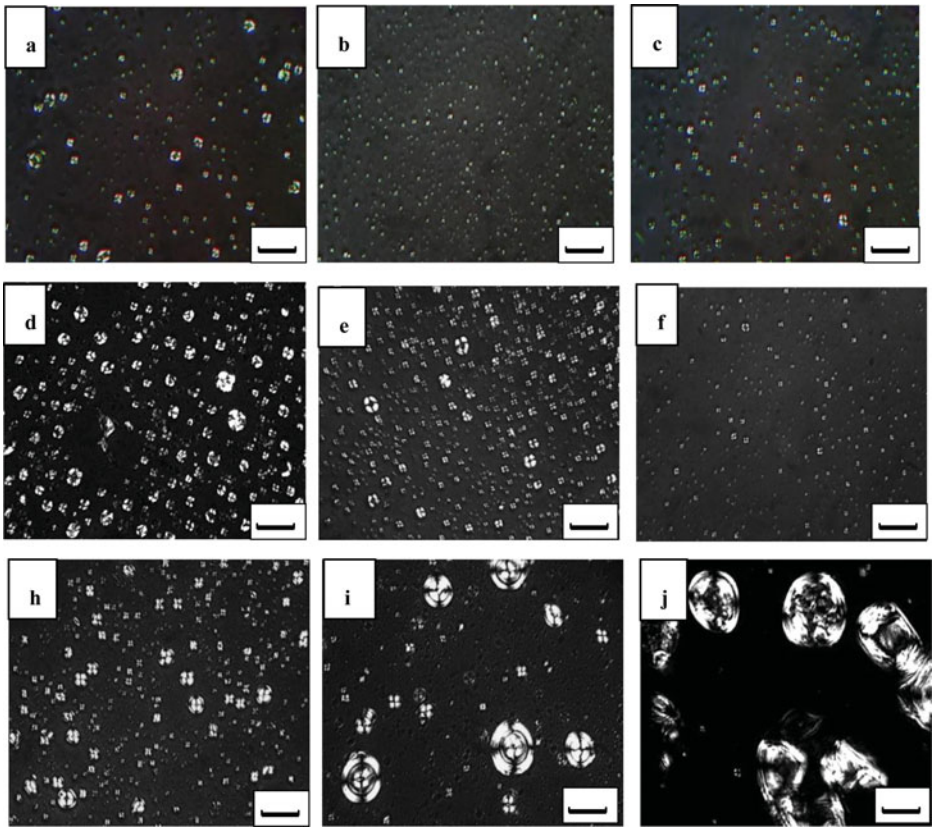

Figure 2. Polarization micrographs at different conditions:70°C,80°C, 90°C(a–c);co-emulsifier of GMS, ceteareth-20 and steareth-21(d-f);different concentration of NaCl:0.05 mol,0.07 mol,0.1 mol(h–j),respectively. Scale bar: 20 μm.

Figs. 2h–j show that concentration of sodium chloride (NaCl) significantly affects the configuration of liquid crystals. When the concentration is 0.05 mol, a characteristic radial texture is observed. However, with the increase in the concentration of NaCl, the shell of lamellar mesophase is observed. When the molecular anchoring is normal at both the inner and outer confining surfaces, the inner drop plays the role of a radial hedgehog. With the further increase in the concentration, the inner drop is not in the center of the larger drop. Instead the nematic elasticity drives the inner drop toward one of the two peripheric boojums (surface point defects) resulting in an inhomogeneous shell thickness [30].

3.2. Characterization of solid lipid microparticles with liquid crystal

3.2.1. Morphology characterization

ESEM showed spherical particles with an irregular fragment, smooth surface and micrometer size, as seen in Fig. 3. It further showed that the particle diameters of solid lipid microparticles vary from about 4 to 6 μm and was in agreement with the DLS studies.

3.2.2. Characterization by X-ray diffraction

The structures of SLMs were measured by X-ray diffraction. The formation of SLM contains aqueous phase and the oil phase (C_{22}APG, C_{16}-C_{18} Normal Mixed Alcohols as the lipid, the co-emulsifier) while the S21-SLM aqueous phase and the oil phase(C_{22}APG, C_{16}-C_{18}

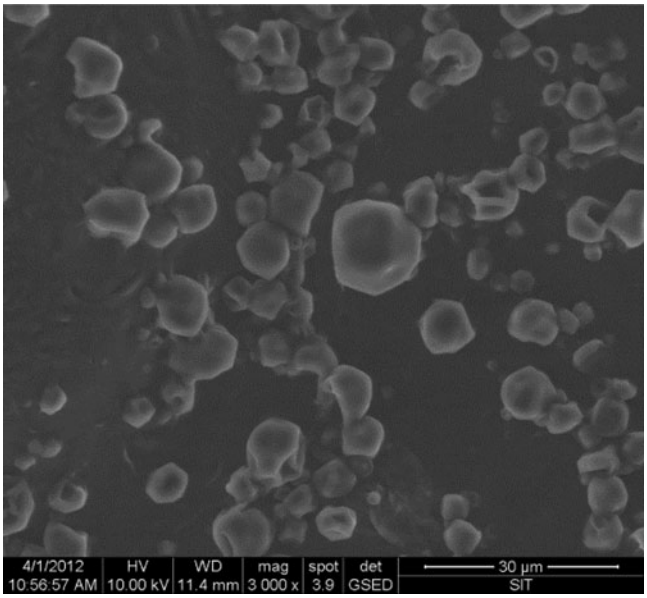

Figure 3. Scanning electron micrographs of solid lipid microparticles (×30,000).

Normal Mixed Alcohols as the lipid, the co-emulsifier) contains aqueous phase and the oil phase(C_{22}APG, C_{16}-C_{18} Normal Mixed Alcohols as the lipid, the co-emulsifier steareth-21). The results are shown in Fig. 4.

The liquid crystal structure was keep to Bragg's equation:

$$d = \lambda/2 \sin\theta$$

in which λ is the wavelength of X-ray scattering, θ is the scattering angle of the incident ray, d is the distance between the lattice layer. When the distance of the liquid crystal layer d for the primary and the senior accords with$d_1 : d_2 : d_3 : d_4 = 1 : 1/2 : 1/3 : 1/4$, the structure is lamellar; When$d_1 : d_2 : d_3 : d_4 = 1 : \sqrt{1/3} : \sqrt{1/4} : \sqrt{1/7}$, the structure belongs to hexagonal; When$d_1 : d_2 : d_3 : d_4. = 1 : \sqrt{1/2} : \sqrt{1/6} : \sqrt{1/10}$, the structure belongs to cubic [31].

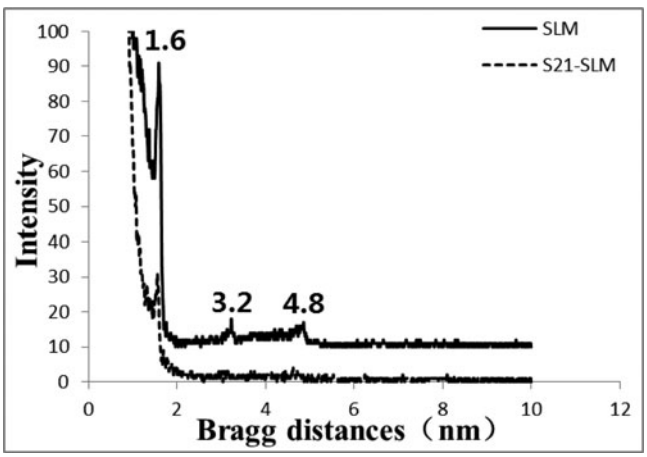

Figure 4. X-ray diffraction curves of SLM and S21-SLM.

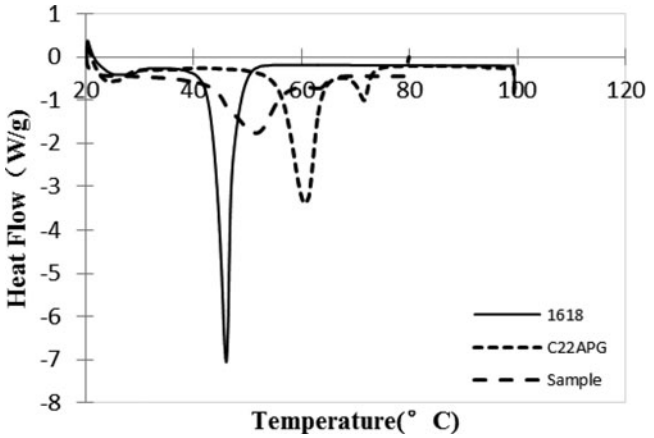

Figure 5. The DSC curves of the 1618,C22APGand the sample.

Fig. 4 shows three main peaks at 1.6, 3.2, and 4.8 nm. Clearly, d1:d2:d3=1:1/2:1/3, and can define that the structure is lamellar.

3.2.3. Characterization by DSC

Differential scanning calorimetry (DSC) is frequently used to measure the heat loss or gain resulting from physical or chemical changes within a sample as a function of the temperature. It has been used to characterize the state and the crystallinity of SLMs. Thermodynamics stability of solid lipid particles relies on their existing lipid modification. DSC uses the fact that different lipid modifications possess different melting points and melting enthalpies. After heated, some hidden information of sample crystal lattice resolution could be showed in DSC curve, such as the melting point, crystallization order, co-crystal mixture. The crystalline index (CI [%]) which is defined as the percentage of the lipid matrix that has recrystallized during storage time was calculated by applying the following equation:

$$\mathrm{CI}\ (\%) = \left(\frac{\Delta H_{SLMs}}{\Delta H_{\text{bulk material}} \times \text{Concentration}_{\text{Lipid}}} \right) \times 100,$$

where, ΔH is the melting enthalpy (J/g) and that can be obtained from the area under the DSC curve of the melting endotherm.

Fig. 5 shows the DSC curves of 1618, C22APG, and the sample of microparticles with liquid crystal recorded from 20∼100°C at a rate of 10°C min^{-1}. The values of related data of peaks and enthalpy are listed in Table 1. The pure 1618 demonstrated a single sharp endothermic peak at approximately 46.11°C. Compared to 1618, C22 APG showed a significant sharp peak at 59.97°C and a shoulder peak at higher temperature at 71.8°C. In general, C22 APG is known to the existence of the isomers such as the glycoside isomers and glycoside isomers. Compared to bulk 1618, the developed formulation developed showed a broadening peak. Both melting

Table 1. DSC parameters of sample, the solid lipid of 1618, and C22 APG.

	Melting point(°C)	Onset point (°C)	Enthalpy(J/g)	CI%
1618	46.11	30.19	133.0	100
C22APG	59.97	26.61	—	—
	71.58	69.93	—	—
Sample	50.31	25.36	34.98	26.30

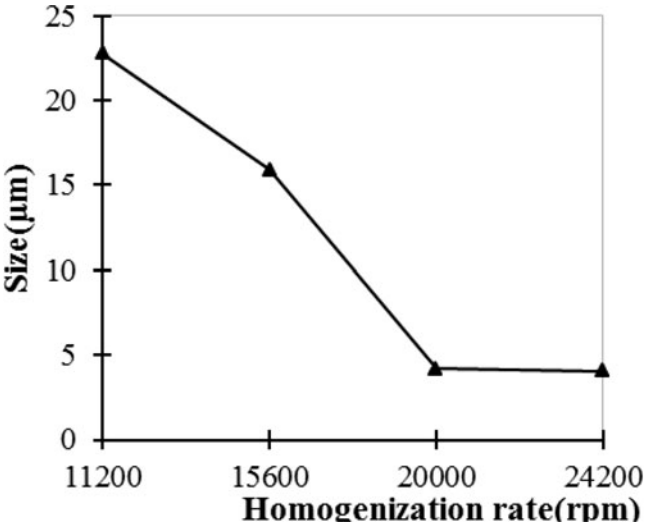

Figure 6. The impact of the homogenization rateon particle size.

point and crystallinity(CI) of 1618 in the formulation decreased. This melting point depression is described by the Gibbs–Thomson equation [32] which indicates that the melting point of the microparticles is always smaller than the melting point of the bulk lipid. These changes indicated the formation of the solid lipid particles from the emulsifier and the lipid. The CI was about 26.3%, indicating that the dominantly physical state consist of less ordered arrangement crystals. There was no clear change in the melting point of the raw materials if they were only physically mixed [33,34].

3.3. Factors influence on particle size

3.3.1. Homogenization rate

Rate of homogenization significantly influenced the particle size.Fig. 6 exhibits that particle size significantly decreased with increasing homogenization rate. When the increase in the homogenization rate from 11,200 rpm to 20,000 rpm, the particle size decreased from 22.287 to 4.210 μm. The size continues to decrease as the emulsion was homogenized at 24,200 rpm; however, further reduction in size is fairly modest. Thus, rate of homogenization was responsible for final particle size, which resulted in the breaking of the coarse emulsion drops to micrometer droplets. Larger homogenization power provided more energy to the dispersions, which reduced the size of the droplets.

3.3.2. Emulsification temperature

The emulsifier temperatures 70, 80, and 90°C were selected to investigate the effect of temperature on the particle size, as shown in Fig. 7.The particle size is about 12 μm when the emulsification is performed at 70°C; however, the particle size is only 4.2 μm at 80°C. The low temperature was propitious to form larger particle, which might contribute to the dispersion of particles. The emulsification temperature affected the viscosity of disperse phase. The higher emulsification temperature resulted in lower viscosity. The low temperature and high viscosity could limit the molecular motion. Moreover, a sharp decrease of temperature during the homogenization process could further lead to the agglomeration of lipid. At high

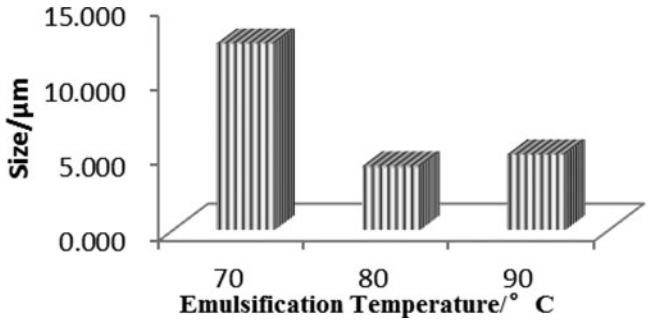

Figure 7. The effect of emulsification temperature on the particle size.

temperature, the emulsifier and lipid could contact completely. Therefore, during the emulsification process, the small particles were apt to form and agglomeration was inhabited. However, higher temperature would affect the interfacial film strength.

3.3.4. Co-emulsifier type and concentration

The co-emulsifier can adjust the hydrophilic–lipophilic-balance value (HLB) of the system, therefore, the type and concentration of the co-emulsifiers significantly affect the quality of microparticles with liquid crystal structure. A wide variety of different emulsifiers can act as the co-emulsifier in this system. In the present study, the influence of three co-emulsifiers, namely, GMS, steareth-21, and ceteareth-20 on particle size and formulation of liquid crystal was examined. In the formulations, C22APG was the main emulsifier and the concentration was 3% (w/w) with 1.5% (w/w) cetostearyl alcohol as the solid lipid.

Fig. 8 clearly demonstrates that the type and concentration of co-emulsifier present in the system significantly influence the size of microparticles. At 1% (w/w) co-emulsifier, the particles with sizes 2.795, 10.334, and 15.350 μm are produced for steareth-21, ceteareth-20, and GMS, respectively. In general, steareth-21 co-emulsifier was in favor of the formulation of

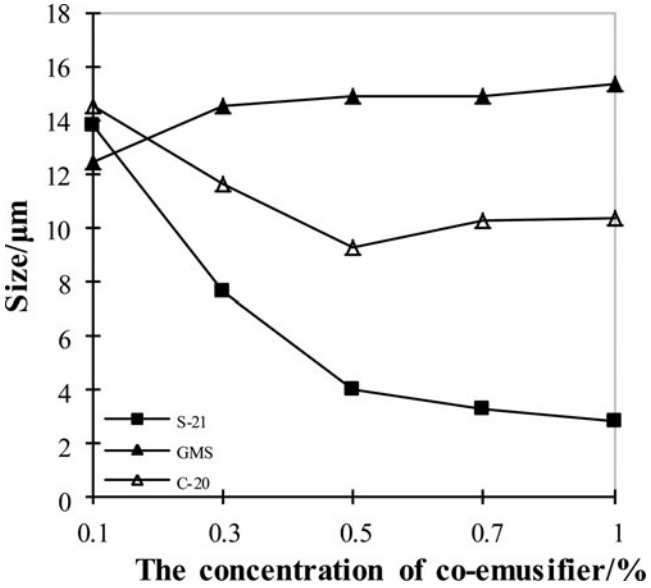

Figure 8. The impact of the type and concentration of co-emulsifier on particlesize.

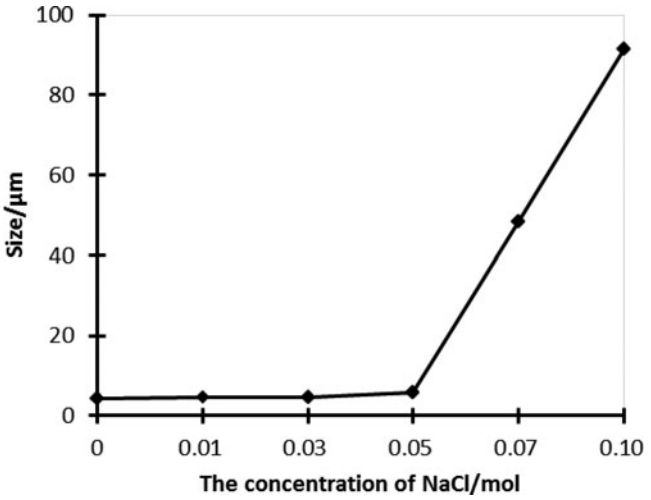

Figure 9. The effect of the concentration of NaCl on the particle size.

smaller size particles. This result was attributed to the HLB of the co-emulsifiers. Kovacevic reported that the HLB of stabilizer influenced the stability of solid lipid particles. The HLB of the emulsifiers should match the required HLB of the inner phase as close as possible. The emulsifiers (main emulsifiers and co-emulsifiers) used in this study possessed different HLB and their values were 15.5, 15.2, 3.8, and 14–16 for steareth-21, ceteareth-20, GMS, and C22APG, respectively. For the solid lipid used in this study, the required HLB was 15.5. When the GMS co-emulsifier compounded with C22APG, the HLB of emulsifiers of system decreased and the desired HLB of lipid could not be achieved. Thus, the GMS did not favor the particle distribution.

Steareth-21 and ceteareth-20 resulted in an apparent decrease in particle size with increasing concentration. First, the addition of co-emulsifiers could result in the HLB of 15.5. Further, with the increase in the concentration, the droplet surfaces would be covered more rapidly by a layer of emulsifier molecules. Thus, high concentrations of the emulsifier reduced the surface tension and facilitated the particle partition during homogenization. However, when the concentration of ceteareth-20 increased from 0.5 to 1%, the particle size decreased from 3.988 to only 2.795 μm. In case of steareth-21, the particle size changed from 9.286 to 10.334 μm, which was considered to be unchanged within the permissible error range. These outcomes indicated that the particle size was limited by other factors such as the maximum disruptive forces and the concentration of the main emulsifier.

For GMS, an actual increase in the particle size was observed with increasing emulsifier content. This was attributed to the influence of aforesaid HLB. When the concentration was increased from 0.1 to 0.3%, the particle size exhibited a clear increase from 12.446 to 14.501 μm. However, when the concentration was continued to increase, the change in the particle size was insignificant. This phenomenon is ascribed to the fact that GMS is the W/O co-emulsifier, which results in an increase in the surface tension.

3.3.5. NaCl concentration

The added salt considerably affects the balance of various inter-bilayer interactions. Therefore, in this study, effect of different concentrations of NaCl on the particle size and structure of liquid crystal was investigated comprehensively. Fig. 9 exhibits the influence of the concentration of NaCl on the particle size. With the addition of low concentration of NaCl, such

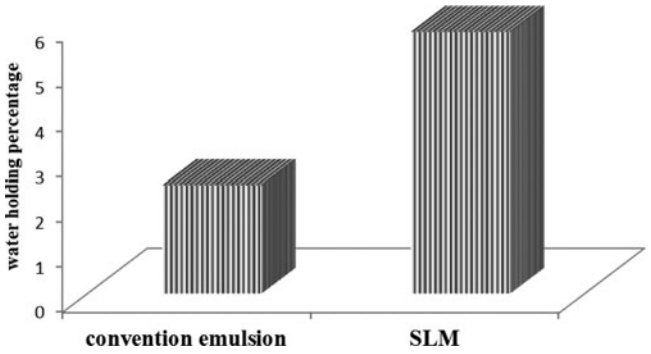

Figure 10. Water content of convention emulsion and SLM.

as 0.01, 0.03, and 0.05 mol, the mean particle size changes insignificantly. Further increase in the NaCl concentration results in the extensive particle aggregation and contributes to the increase in particle size. The aggregation of particles is influenced by the Van der Waals interactions and electrostatic repulsion. The system was formulated by the non-ionic surfactant. Addition of NaCl led to a change in the charge, which increased the electrostatic repulsion between the particles. At lower concentration of NaCl, the electrostatic repulsion was still strong enough to overcome the Van der Waals interactions. When the concentration was more than 0.05 mol, the diffuse electric double layer would be compressed and the Van der Waals interactions contributed to the aggregation of particles.

3.4. In vitro water content investigation

A convention emulsion composed of Span 80, Tween 80, and GTCC was prepared. Notably, the convention emulsion and SLMs would be different in composition. Karl Fischer titration was used to determine the water content between the lamellar liquid crystalline.

Fig. 10 shows the water-holding capacity of each sample. The water holding capacity of SLM emulsion was 5.8%; however, that of the convention emulsion was 2.4%. Obviously, the SLM emulsion had a higher water holding capacity than the convention emulsion. This indicated that some of the water sandwiched between the oil phases was chemically bound by the lamellar structure.

4. Conclusions

This study had shown that the solid lipid microparticles with liquid crystal can be prepared by C22 APG and 1618 alcohol. ESEM showed spherical particles with an irregular fragment, smooth surface and micrometer size. The liquid crystal structure of the particles was lamellar by X-ray diffraction. And SLMs had single crystal structure as evidenced by the appearance of a thermal transition peak in the DSC.A number of important factors that influence the particle size were identified. In order to observe the smaller particle size, the optimal process variables of homogenization rate at 20,000 rpm and homogenization temperature at 80°C. Steareth-21 favored the emulsification and particle size significantly decreased with increasing the concentration. When the concentration of NaCl was more than 0.05 mol, the particle size increased rapidly and the shell of lamellar mesophase began to present. SLMs had a higher water holding capacity than convention emulsion due to the lamellar structure. The result indicated that the SLMs with liquid crystal were steady.

Acknowledgment

The authors would like to thank Mrs. Hu Jing for the DSC measurements.

Statement

The manuscript has not been published elsewhere and that it has not been submitted simultaneously for publication elsewhere. Authors are responsible for obtaining permission to reproduce copyrighted material from other sources and are required to sign an agreement for the transfer of copyright to the publisher.

References

[1] Wojtowicz, P. J., Sheng, P., & Priestley, E. (1975). *Introduction to Liquid Crystals*. Springer: Berlin.
[2] Demus, D., Goodby, J. W., Gray, G. W., Spiess, H. W., & Vill, V. (2011). *Handbook of Liquid Crystals, Low Molecular Weight Liquid Crystals I: Calamitic Liquid Crystals*. John Wiley & Sons: New York.
[3] Jin, L., Zeng, Z., & Huo, Y. (2010). *J. Mech. Phys. Solids*, *58*(11), 1907–1927.
[4] Zheng, M., Wang, Z., Liu, F., Mi, Q., & Wu, J. (2011). *Coll. Surf. A: Physicochem Eng. Aspects*, *385*(1–3), 47–54.
[5] Rades, T., & Müller-Goymann, C. (1997). *Int. J. Pharm*, *159*(2), 215–222.
[6] Ko, S. Y., & Dalvit,C. (1992). *Int. J. Pept. Prot. Res.*, *40*(5), 380–382.
[7] Stevenson, C. L., Bennett, D. B., & Lechuga-Ballesteros, D. (2005). *J. Pharm. Sci.*, *94*(9), 1861–1880.
[8] Savic, S., Lukic, M., Jaksic, I., Reichl, S., Tamburic, S., & Müller-Goymann, C. (2011). *J. Coll. Interf. Sci.*, *358*(1), 182–191.
[9] Sonoda, T., Takata, Y., Ueno, S., & Sato, K. (2006). *Cryst. Growth Des.*, *6*(1), 306–312.
[10] Rodríguez-Abreu, C., & Lazzari, M. (2008). *Curr. Opin. Coll. Interf. Sci.*, *13*(4), 198–205.
[11] Mosca, M., Murgia, S., Ceglie, A., Monduzzi, M., & Ambrosone, L. (2006). *J. Phys. Chem. B*, *110*(51), 25994–26000.
[12] Pople, P. V., & Singh, K. K. (2006). *AAPS PharmSciTech*, *7*(4), E63–E69.
[13] Pardeike, J., Hommoss, A., & Müller, R. H. (2009). *Int. J. Pharm.*, *366*(1), 170–184.
[14] Müller, R., Runge, S., Ravelli, V., Thünemann, A., Mehnert, W., & Souto, E. (2008). *Eur. J. Pharm. Biopharm.*, *68*(3), 535–544.
[15] Muller, R. H., Mader, K., & Gohla, S. (2000). *Eur. J. Pharm. Biopharm.*, *50*, 161–178.
[16] Priscilla, C. H. W., Paul, W. S. H., & Lai, W. C. (2015). *Mol. Pharm.*, *12*, 1592–1604.
[17] Fernando, E. M., Marcello, D. S., & Nadia, P., et al. (2015). *Food Res. Int. l*, *67*, 52–59.
[18] Vivek, R. Y., Sarasija, S., & Kshama, D., et al. (2009). *J. Pharm. Pharmacol.*, *61*, 311–321.
[19] Das, S., Ng, W. K., Kanaujia, P., Kim, S., & Tan, R. B. (2011). *Coll. Surf. B: Biointerf.*, *88*(1), 483–489.
[20] Priscilla, C. H. W., Paul, W. S. H., & Lai, W. C. (2015). *Mol. Pharm.*, *12*, 1592–1604.
[21] Fernando, E. M., Marcello, D. S., & Nadia, P., et al. (2015). *Food Res. Int.*, *67*, 52–59.
[22] Vivek, R. Y., Sarasija, S., & Kshama, D., et al. (2009). *J. Pharm. Pharmacol.*, *61*, 311–321.
[23] Joshi, M. D., & Müller, R. H. (2009). *Eur. J. Pharm. Biopharm.*, *71*(2), 161–172.
[24] Andrade, F. F., Santos, O. D. H., & Oliveira, W. P., et al. (2007). *Int. J. Cosmetic Sci.*, *29*, 211–218.
[25] Zhang, S., Yun, J., Shen, S., Chen, Z., Yao, K., Chen, J., & Chen, B. (2008). *Chem. Eng. Sci.*, *63*(23), 5600–5605.
[26] Attama, A. A., & Igbonekwu, C. N. (2011). *Asian Pac. J. Trop. Med.*, *4*(4), 253–258.
[27] Attama, A., & Müller-Goymann, C. (2007). *Int. J. Pharm.*, *334*(1), 179–189.
[28] Reithmeier, H., Hermann, J., & Gopferich, A. (2001). *Int. J. Pharm.*, *218*, 133–143.
[29] Kato, T. (2002). *Science*, *295*, 2414–2418.
[30] Simon, K. A., Sejwal, P., Gerecht, R. B., & Luk,Y.-Y. (2007). *Langmuir*, *23*(3), 1453–1458.
[31] Tao, J., Zhong, J., Liu, P., Daniels, S., & Zeng, Z. (2012). *J. Fluorine Chem.*, *144*, 73–78.
[32] Lopez-Leon, T., & Fernandez-Nieves, A. (2011). *Coll. Polym. Sci.*, *289*(4), 345–359.
[33] Han, F., Li, S., Yin, R., Liu, H., & Xu, L. (2008). *Coll. Surf. A: Physicochem. Eng. Aspects*, *315*(1), 210–216.
[34] Laura, C., Milena, S., Giovanna, B., Cristina, B. M., Giuseppina, S., & Giampiero, B. (2013). *J. Thermal Anal. Calorimetry*, *111*(3), 2149–2155.